






Numerical Modeling of Complex Geometry Thin Composite Structures under Vibrational Testing

Stepan A. Lavrenkov¹ , Ivan E. Smirnov¹ ,
Dmitrii A. Kravchenko^{1,2} , Katerina A. Beklemysheva¹ ,
Alexey V. Vasyukov¹ 

© The Authors 2024. This paper is published with open access at SuperFri.org

This paper considers the inverse problem of material elastic properties identification from vibrational testing data. The present work aims to describe the approach that uses different kinds of optimizations to allow fast inverse problem solution using single modern multicore CPU or GPU. This includes choosing the model that allows to minimize the computational cost still reproducing the experimental results with good quality. The model for mid-surface symmetric isotropic and composite plates that are moving in vibrational stand is provided. The inverse problem is formulated in terms of the loss function minimization and the solution is computed with stochastic global optimization algorithm and second-order local optimization algorithm, which uses automatic differentiation of the forward problem solver to compute the derivatives. The paper describes parallelization for CPU and GPU and also the approach to reduce RAM usage to fit into single server RAM or single GPU VRAM. The numerical experiments presented in the paper demonstrate the solutions for complex rheologies and geometries: laminated composite plates, isotropic materials with frequency dependent elastic properties, perforated samples.

Keywords: inverse problem, vibrational testing, automatic differentiation, openmp, jar.

Introduction

This paper considers the inverse problem of material elastic properties identification from vibrational testing data. Inverse problems are typically very computationally intensive. They are commonly solved using large scale clusters to achieve high quality of the solution. However, for the problem we consider, it is desirable to fit into simple hardware setup. If the problem can be solved using a single computer, the solver can be taken close to vibrational testing stands and integrated into engineering procedures. The present work aims to describe the approach that uses different kinds of optimizations to allow fast inverse problem solution using modern multicore CPU or GPU.

Composite materials are widely used in modern engineering projects, sometimes new materials are tailor-made for a certain problem. The experimental status of such materials may lead to lack of reliable data on their elastic properties, that are crucial for engineering estimations and numerical simulations. Moreover, even if the elastic properties of the material are considered to be known, an exact specimen may have different kinds of flaws caused by issues during the material production and further handling. The present work uses the data from the vibrational testing of the specimen to identify its elastic properties. The results of this work will contribute to the methods of nondestructive testing. The choice of the input data is based on the fact that vibrational testing is a routine procedure in many areas. So, if the vibrational data is available, it is desirable to get an additional information from this data. It is worth noting that the target problem of this paper should not be confused with nondestructive health monitoring methods based on known vibration signatures.

¹Moscow Institute of Physics and Technology, Dolgoprudny, Russia

²Keldysh Research Center, Moscow, Russia

Similar problems were considered by different groups of authors. The paper [9] presented an approach that is very close to the one we used, but the authors simulated the response of a beam specimen, and we consider plates. Completely different approaches exist also, the one to mention is Dynamic Mechanical Analysis [2], but it requires small samples of the material of certain shapes, and it is not an option for our use case.

The approach used in this work is based on the results presented earlier by several authors. The work [24] used the experimental stand similar with the one referred to in the present work, the authors measured a mechanical impedance of a triangular aluminum plate in an atmosphere and in a vacuum chamber to study an energy dissipation processes. In [23] the different models for damping in composite materials are overviewed. Several works showed that different materials may have significantly different frequency dependencies of elastic properties [10, 15–17]. The usage of frequency-dependent dynamic moduli in [21] provided better explanation of a dynamic behaviour of a specimen made of two steel plates connected by a polymer layer. In [4] a framework is suggested, which allows to introduce into the model the phenomena of viscous, thermoelastic and viscoelastic damping and the damping due to sound radiation. The exact approach we use was first introduced in [1], the present work extends it and adapts to more complex rheologies and geometries.

The paper is structured as follows. Section 1 covers the choice of the model that allowed to minimize the computational cost still reproducing the experimental results with good quality. Section 2 describes the algorithmic approaches taken that allowed for effective parallelization both on CPU and GPU. The algorithmic part also covers the approach to reduce RAM usage to fit into single server RAM or single GPU VRAM. Section 3 presents the computational results to demonstrate the quality of the solution for complex rheologies and geometries.

1. Mathematical Model

In present work we consider the boundary value problem for the equation of motion of thin plate in the given experimental setup. One edge of the plate is clamped in the vibration stand, which generates sinusoidal oscillations with adjustable frequency, another edge is free. Both edges of the plate have the accelerometers installed on them, which allows for experimental acquisition of frequency-response function of plate oscillations. The forward problem is formulated as follows: *obtain frequency response for the plate with known properties*. Consequently, the inverse problem is *to compute the unknown elastic moduli of the material from experimentally obtained frequency response and geometrical properties of the plate*.

1.1. Forward Problem

The equations of motion for the plate was derived using the following assumptions:

- the plate is thin, so its height is much less than its length and width;
- the Kirchhoff-Love kinematic hypothesis is applicable: straight lines normal to the mid-surface remain straight and normal to the mid-surface after deformation, the thickness of the plate does not change during a deformation;
- the plate is symmetric with respect to the mid-surface and has the same height for every in-plane point;
- if the plate consists of several laminae, each lamina has constant thickness.

The resulting equations of motion are [19]:

$$2e\rho\ddot{w}(x, y, t) - \frac{2e^3}{3}\rho\Delta\ddot{w}(x, y, t) + \nabla \cdot \nabla \cdot \mathbf{M}(x, y, t) = 0, \quad (x, y) \in \Omega,$$

where w is the transverse movement of the plate, $e = \frac{1}{2}h$ is half of the plate thickness, Ω is a non-empty connected open subset of \mathbb{R}^2 , which represents mid-surface of a plate, ρ is the density of the material, \mathbf{M} is the tensor of moments:

$$\begin{pmatrix} M_{xx} & M_{xy} \\ M_{xy} & M_{yy} \end{pmatrix} = \int_{-e}^e \begin{pmatrix} \sigma_{xx} & \sigma_{xy} \\ \sigma_{xy} & \sigma_{yy} \end{pmatrix} z^2 dz.$$

For a linear elastic material:

$$\begin{pmatrix} M_{xx} \\ M_{yy} \\ M_{xy} \end{pmatrix} = \begin{pmatrix} D_{11} & D_{12} & D_{16} \\ D_{12} & D_{22} & D_{26} \\ D_{16} & D_{26} & D_{66} \end{pmatrix} \begin{pmatrix} \frac{\partial^2}{\partial x^2} w \\ \frac{\partial^2}{\partial y^2} w \\ \frac{\partial^2}{\partial x \partial y} w \end{pmatrix} = D \begin{pmatrix} 1 & \nu & 0 \\ \nu & 1 & 0 \\ 0 & 0 & \frac{1-\nu}{2} \end{pmatrix} \begin{pmatrix} \frac{\partial^2}{\partial x^2} w \\ \frac{\partial^2}{\partial y^2} w \\ \frac{\partial^2}{\partial x \partial y} w \end{pmatrix},$$

where $D = \frac{Eh^3}{12(1-\nu^2)}$ is flexural rigidity, $\nu = (\frac{E}{2G} - 1)$ is Poisson's ratio, E is Young's modulus, G is shear modulus.

In case of laminated plates the classical laminate theory (CLT) [8, 19] is used to determine D_{ij} components. In present work, orthotropic laminae are considered. Consider the k -th orthotropic lamina with axes $(x_1, y_1)_k$ which are associated with the transverse and normal directions to the reinforcing fibers. These axes are rotated by angle φ_k counterclockwise about the plate axes (x, y) . In $(x_1, y_1)_k$ axes Hooke's law is formulated as:

$$\begin{pmatrix} \sigma_1 \\ \sigma_2 \\ \sigma_6 \end{pmatrix}_k = \begin{pmatrix} Q_{11} & Q_{12} & Q_{16} \\ Q_{12} & Q_{22} & Q_{26} \\ Q_{16} & Q_{26} & Q_{66} \end{pmatrix}_k \begin{pmatrix} \varepsilon_1 \\ \varepsilon_2 \\ \varepsilon_6 \end{pmatrix}_k, \quad (1)$$

where Q_{ij} are components of tensor \mathbf{Q}_k which depend on engineering constants $E_1, E_2, G_{12}, \nu_{12}$:

$$\nu_{21} = \frac{E_2\nu_{12}}{E_1}, \quad Q_{11} = \frac{E_1}{1 - \nu_{12}\nu_{21}}, \quad Q_{22} = \frac{E_2}{1 - \nu_{12}\nu_{21}}, \quad Q_{12} = \nu_{12}Q_{22},$$

$$Q_{66} = G_{12}, \quad Q_{16} = Q_{26} = 0.$$

The equation (1) in (x, y) axes:

$$\begin{pmatrix} \sigma_{xx} \\ \sigma_{yy} \\ \sigma_{xy} \end{pmatrix}_k = \begin{pmatrix} \overline{Q}_{11} & \overline{Q}_{12} & \overline{Q}_{16} \\ \overline{Q}_{12} & \overline{Q}_{22} & \overline{Q}_{26} \\ \overline{Q}_{16} & \overline{Q}_{26} & \overline{Q}_{66} \end{pmatrix}_k \begin{pmatrix} \varepsilon_{xx} \\ \varepsilon_{yy} \\ \gamma_{xy} \end{pmatrix}_k. \quad (2)$$

Here $\overline{\mathbf{Q}}_k = \mathbf{T}(\varphi_k) \cdot \mathbf{Q}_k \cdot \mathbf{T}^T(\varphi_k)$, rotational tensor \mathbf{T} in (x, y) axes:

$$\mathbf{T}(\varphi_k) = \begin{pmatrix} \cos^2 \varphi_k & \sin^2 \varphi_k & -2 \sin \varphi_k \cos \varphi_k \\ \sin^2 \varphi_k & \cos^2 \varphi_k & 2 \sin \varphi_k \cos \varphi_k \\ \sin \varphi_k \cos \varphi_k & -\sin \varphi_k \cos \varphi_k & \cos^2 \varphi_k - \sin^2 \varphi_k \end{pmatrix}.$$

The D_{ij} components for the laminate with N laminae are then calculated as

$$\mathbf{D} = \begin{pmatrix} D_{11} & D_{12} & D_{16} \\ D_{12} & D_{22} & D_{26} \\ D_{16} & D_{26} & D_{66} \end{pmatrix} = \sum_{k=1}^N \int_{z_{k-1}}^{z_k} \begin{pmatrix} \overline{Q}_{11} & \overline{Q}_{12} & \overline{Q}_{16} \\ \overline{Q}_{12} & \overline{Q}_{22} & \overline{Q}_{26} \\ \overline{Q}_{16} & \overline{Q}_{26} & \overline{Q}_{66} \end{pmatrix}_k z^2 dz. \quad (3)$$

In the equation above, z corresponds to a coordinate along axis, which is normal to the mid-surface. Also, the following rule is applied: $z_0 = -e$, $z_N = e$, $z_k - z_{k-1} = h_k$ - thickness of k -th lamina. Each lamina is orthotropic and has constant thickness across the plate so the general formula is:

$$D_{ij} = \frac{1}{3} \sum_{k=1}^N (\overline{Q}_{ij})_k (z_k^3 - z_{k-1}^3).$$

Considering the oscillations as harmonic $w = u(x, y, \omega)e^{i\omega t}$ and introducing the damping via complex dynamic moduli [12] with loss factor β such as $\mathcal{D}_{ij} = D_{ij}(1 + i\beta)$, we arrive at the equation of motion in frequency domain (4) with boundary conditions (5) on the clamped end, which oscillates with amplitude g_0 , and (6) on the free end [20].

$$-2e\rho\omega^2 \left(u - \frac{e^2}{3} \Delta u \right) + \nabla \cdot \nabla \cdot (\mathcal{D} \cdot \nabla \otimes \nabla u) = 0, \quad (4)$$

$$\begin{cases} u = g_0 \\ \nabla u \cdot \mathbf{n} = 0 \end{cases} \quad (x, y) \in \Gamma_c, \quad (5)$$

$$\begin{cases} -\frac{2}{3}e^3\rho\omega^2 \nabla u \cdot \mathbf{n} + \nabla \cdot \mathbf{M} \cdot \mathbf{n} + \nabla(\mathbf{M} \cdot \mathbf{n} \cdot \boldsymbol{\tau}) \cdot \boldsymbol{\tau} = 0 \\ \mathbf{M} \cdot \mathbf{n} \cdot \boldsymbol{\tau} = 0 \end{cases} \quad (x, y) \in \Gamma_f. \quad (6)$$

1.2. Inverse Problem

Let θ be the vector of unknown model parameters (for an isotropic material $\theta = (E, G, \beta)^\top$, for an orthotropic one $\theta = (E_1, E_2, G_{12}, \nu_{12}, \beta)^\top$, and $\{(\omega_k, u_k^{exp})\}_{k=1}^N$ - discrete frequency response acquired in the experiment. Then, solving the inverse problem is equal to finding the minimum of a loss function (7)

$$L(\theta_s) = \min_{\theta \in \Theta} L(\theta) = \min_{\theta \in \Theta} \left[\frac{1}{N_{exp}} \sum_{m=1}^{N_{exp}} (\log(|u(\omega_m, \theta)|) - \log(|u_{exp}(\omega_m)|)) \right], \quad (7)$$

where $u(\theta, \omega_k)$ is a solution of a forward problem with parameters θ and frequency ω_k , Θ is the admissible set of parameters, θ_s is a solution vector.

2. Numerical Method and Algorithms

2.1. Forward Problem

The system of equations (4)–(6) is solved numerically using FEM with Morley elements [13]. The matrices obtained after spatial discretization are not dependent on frequency ω and tensor \mathcal{D} . This makes the following optimization possible: matrices are calculated once and stored in memory, so the global matrix of linear system is obtained via linear combination with coeffi-

cients, which depend on ω and values in tensor \mathcal{D} . So, forward problems for different vectors of unknowns θ can be solved independently using parallel computations.

The algorithm described above was implemented in Python using FreeFem++ [7] for FEM matrices operations and jax [3] for automatic differentiation of forward problem solver and JIT compilation for CPU and GPU targets. In present, work two implementations were used. The first one is GPU-accelerated solver which is based on dense matrix operations provided by jax. The second solver uses CPU to operate on sparse matrices. After FEM discretization the sparsity pattern of the resulting linear system is determined so all constant matrices are stored as 1D arrays. This solver uses UMFPACK [6] to solve the resulting sparse linear system and OpenMP [5] to implement parallel computations for linear systems with different frequencies ω .

The computation of forward problem with CPU solver takes around 1.5 seconds on a single core of Intel i7-11370H CPU for a rectangular isotropic plate with reasonably dense spatial mesh and 1000 frequencies. The computation requires around 1.5 GB RAM. The efficiency of the parallel version is about 70%. This allows to achieve forward problem computation time less than 0.5 seconds when using single multi core CPU. These results allow to solve the inverse problem on a single machine as well.

2.2. Inverse Problem

The minimization of loss function (7) is implemented with global and local optimization algorithms. Global optimization uses differential evolution algorithm [22] to find the approximate minimum when the bounds on each parameter are given. Then, local optimization based on trust-region method [14] is used to improve the solution from global optimization. The local optimization uses gradients and Hessian matrices calculated via automatic differentiation. Also, the data compression algorithm [11] is used to decrease the amount of points in discrete frequency range which results in lower RAM consumption.

3. Results

3.1. Composite Laminates

Three numerical experiments were conducted using the algorithm for laminates described above. Plates with lamina from carbon-fiber reinforced polymers (CFRP) were chosen, the reference parameters were taken from [18]. The modeling covered the plate under investigation and also the accelerometer with mass 1.7 g and radius 3.8 mm. The results of numerical simulation may provide a valuable insight on how the experimental procedure could be improved.

3.1.1. Laminate with plies of woven fabric

In this case, the material has reinforcing fibers in two orthogonal directions with plain weave. This symmetry allows for the following simplification: two engineering constants are equal $E_1 = E_2$ and the number of unknown elastic moduli is reduced by one. The parameters of the plate are listed in Tab. 1.

Using these parameters the forward problem was solved in frequency range from 0 to 2500 Hz. The result of this calculation was considered to be the reference data. Then, the parameters of the specimen were considered unknown, and the inverse problem was solved in respect to the reference data. The results are presented in Fig. 1 and in Tab. 2. These results show that the

inverse problem can be solved with high accuracy for such parameter configuration even for really large bounds for global optimization.

Table 1. Woven fabric sample parameters

| Parameter | Value |
|--|----------------|
| Dimensions, [mm] | 100 × 20 × 1.5 |
| Ply orientation, [degrees] | (0, 30, 0) |
| Density ρ , [kg · m ⁻³] | 1400 |
| E_1, E_2 , [GPa] | 61.0 |
| G_{12} , [GPa] | 4.9 |
| ν_{12} , [1] | 0.04 |
| Loss modulus β , [1] | 0.02 |

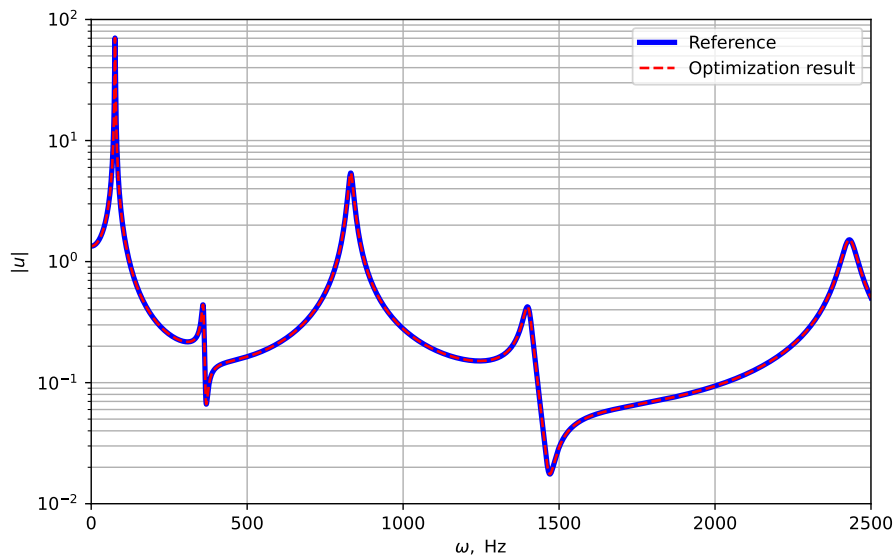


Figure 1. Woven fabric sample: frequency responses for reference parameter values and values from the inverse problem solution

Table 2. Results for plate with woven plies

| Parameter | E_1 , GPa | G_{12} , GPa | ν_{12} |
|--|----------------------|----------------|------------|
| Reference value | 61.0 | 4.9 | 0.04 |
| Parameter bounds for global optimization | 3–130 | 1–40 | 0.01–1.0 |
| Optimization result | 60.99 | 4.899 | 0.0404 |
| Relative error, % | $-2.2 \cdot 10^{-4}$ | -0.014 | 0.9 |

3.1.2. Thin anisotropic plate

In this experiment, the material consists of thin unidirectional plies with the parameters presented in Tab. 3. The forward problem was solved in frequency range from 0 to 2700 Hz. The inverse problem was solved for two different frequency ranges: 0–1700 Hz and 0–2700 Hz. The

results are presented in Fig. 2 and in Tab. 4. The results show that the quality of solution may benefit from narrowing the frequency range in case when there are many peaks present in AFC.

Table 3. Thin sample parameters

| Parameter | Value |
|--|-----------------------------|
| Dimensions, [mm] | $100 \times 20 \times 0.45$ |
| Ply orientation, [degrees] | (0, 35, 0) |
| Density ρ , [$\text{kg} \cdot \text{m}^{-3}$] | 1100 |
| E_1 , [GPa] | 67.4 |
| E_2 , [GPa] | 17.7 |
| G_{12} , [GPa] | 11.34 |
| ν_{12} , [1] | 0.47 |
| Loss modulus β , [1] | 0.02 |

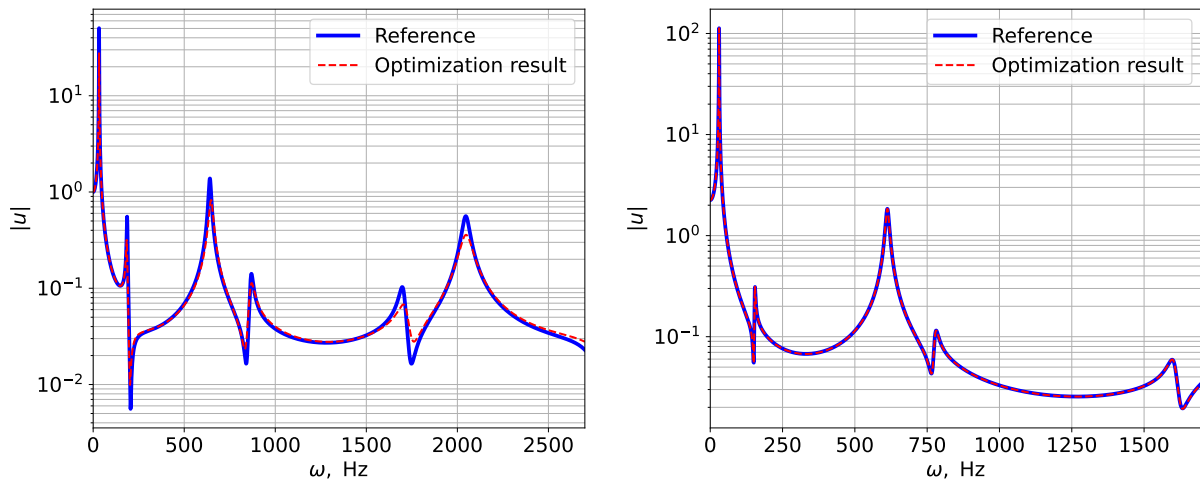


Figure 2. Thin plate: results for wide (left) and narrow (right) frequency ranges

Table 4. Results for thin plate with unidirectional plies in wide/narrow frequency range

| Parameter | E_1 , GPa | E_2 , GPa | G_{12} , GPa | ν_{12} |
|--|-------------|-------------|----------------|------------|
| Reference value | 67.4 | 17.7 | 11.3 | 0.47 |
| Parameter bounds for global optimization | 30–200 | 1–50 | 1–50 | 0.01–2.0 |
| Optimization result | 72.2/68.6 | 17.8/18.1 | 11.4/11.3 | 0.45/0.471 |
| Relative error, % | 7.2/1.8 | 0.7/2.4 | 0.3/0.007 | –3.5/0.2 |

3.1.3. Thick anisotropic plate

In this experiment, the laminate consists of 11 unidirectional plies with the parameters presented in Tab. 5. The forward problem was solved in frequency range from 0 to 2500 Hz. The results are presented in Fig. 3 and in Tab. 6. The relative error of inverse problem solution is higher in comparison to thin plate case, which means that accuracy may decrease for plates with many laminae.

Table 5. Parameters for thick plate

| Parameter | Value |
|--|---|
| Dimensions, [mm] | $100 \times 20 \times 1.4$ |
| Ply orientation, [degrees] | (0, 35, 45, 90, 45, 0, 45, 90, 45, 35, 0) |
| Density ρ , [$\text{kg} \cdot \text{m}^{-3}$] | 1400 |
| E_1 , [GPa] | 62 |
| E_2 , [GPa] | 45 |
| G_{12} , [GPa] | 21 |
| ν_{12} , [1] | 0.42 |
| Loss modulus β , [1] | 0.02 |

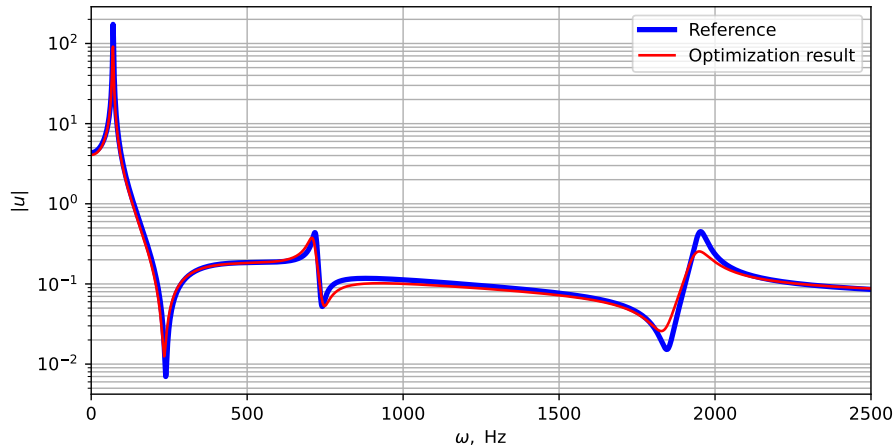

Figure 3. Thick plate: inverse problem solution and reference AFC

Table 6. Results for thick plate

| Parameter | E_1 , GPa | E_2 , GPa | G_{12} , GPa | ν_{12} |
|-------------------------|-------------|-------------|----------------|------------|
| Reference value | 62.0 | 45.0 | 21.0 | 0.42 |
| Bounds for optimization | 3–150 | 10–70 | 1–50 | 0.01–2.0 |
| Optimization result | 63.33 | 47.55 | 21.3 | 0.352 |
| Relative error, % | 2.2 | 5.7 | 1.4 | –16.2 |

3.2. Isotropic Samples

Several numerical experiments were performed for isotropic metallic samples, since real experimental data was available for such specimens. These experiments aim to demonstrate that the presented approach can work for real life samples taking into account relatively complex geometry and rheology.

3.2.1. Frequency dependence

As it was mentioned in Introduction, there are evidences that different materials possess significantly different frequency dependence of elastic moduli. There is no common theory in this area that covers all the materials and frequency ranges. Different authors typically use empirical formulae derived from experimental data. The present work used two most common approaches. The first one is linear increase or decrease of moduli as given by (8). The results

that can be achieved with this approximation are presented in Fig. 4. The change of moduli on 2000 Hz were 30 % of the initial values.

$$\begin{aligned} E &= E_0 (1 \pm \alpha\omega), \\ \nu &= \nu_0 (1 \pm \beta\omega). \end{aligned} \tag{8}$$

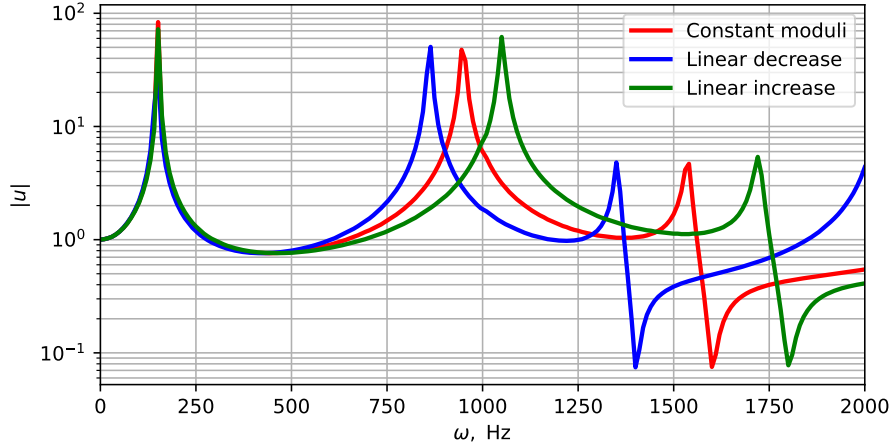


Figure 4. Synthetic calculations with frequency dependent elastic moduli

The second commonly used approximation is expressed as (9). When using the second approximation, $\{\alpha_E, \beta_E, \alpha_\nu, \beta_\nu\}$ become additional sought coefficients of inverse problem. This makes the inverse problem harder but allows to capture more complex material behaviour.

$$\begin{aligned} E &= E_0 \left(1 + \alpha_E e^{\beta_E \omega}\right), \\ \nu &= \nu_0 \left(1 + \alpha_\nu e^{\beta_\nu \omega}\right). \end{aligned} \tag{9}$$

To test this approximation, the inverse problem was solved twice using the real experimental data for a steel plate. The first solution was obtained without taking frequency dependence into account. The second solution was calculated using the approximation (9). The frequency response results are presented in Fig. 5. The final parameters for the solution without frequency dependence are: $\{E = 192.47 \text{ GPa}, \nu = 0.23, \beta = 0.0091\}$. The results for the solution with frequency dependence are presented in Tab. 7. One can see that the frequency dependence for the specimen under testing can be considered neglectable in the frequency range used in the experiment. However, this experiment demonstrated that the solution of the inverse problem remains stable when we introduce frequency dependence of moduli.

Table 7. Results for frequency dependent elastic moduli

| Parameter | α_E | β_E | α_ν | β_ν | E_0 | ν_0 | β |
|-----------|-----------------------|---------------------|----------------------|-------------|--------|---------|---------|
| Value | $-2.57 \cdot 10^{-4}$ | $6.5 \cdot 10^{-4}$ | $-4.0 \cdot 10^{-4}$ | 10^{-3} | 192.47 | 0.23 | 0.0091 |

3.2.2. Perforated plates

Another numerical experiment performed was about testing the possibility to represent highly perforated specimens using effective parameters. The motivation behind this experiment is the fact that calculations of perforated plates with real geometry require a large amount

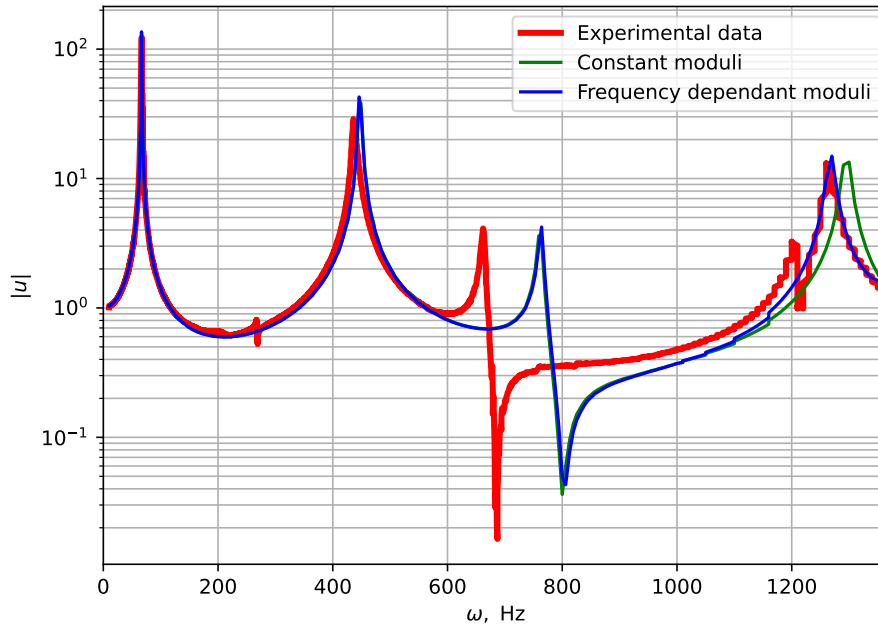


Figure 5. Inverse problem solution with frequency dependence of elastic moduli

of time and memory to represent the holes in details. An example of such perforated plate with generated mesh on it is displayed in Fig. 6. A possible way to solve this problem is to determine effective parameters of solid plate that has the same frequency response function as the perforated one.

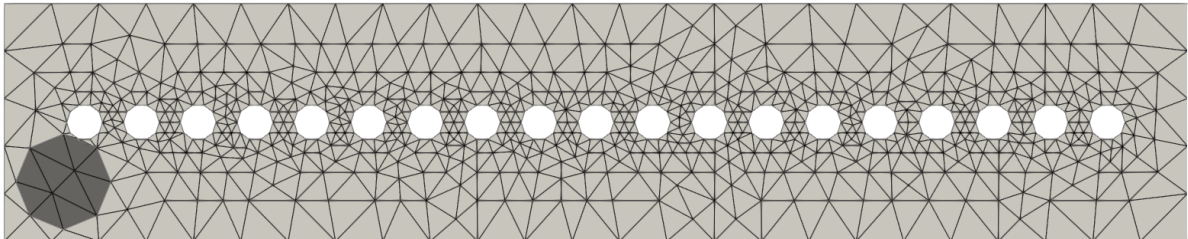


Figure 6. An example of perforated plate with mesh on it

During this experiment, the plate was taken perforated by one central line of holes along length, total linear size of holes was kept constant but their radius was varied. An effective density of a solid plate was calculated as $\rho = \rho_0 (1 - \pi r^2 N / xy)$, where ρ_0 is real material density, r – radius of each hole, N – number of holes, xy – square of plate. An inverse problem was solved for each value of radius to determine effective elastic moduli. The results are presented in Fig. 7, the values are presented relative to the moduli on the solid plate without perforation.

This approach was tested for the inverse problem solution. The results are presented in Fig. 8. Red line represents real experimental vibrational data for 2 mm thick aluminum plate with 19 holes of 1.5 mm radius. Green line is the result of solving the direct problem for a solid plate with an effective density and elastic moduli calculated from the dependence presented in Fig. 7. Blue line is the result of solving the inverse problem for a solid plate using these effective density and elastic moduli as an initial guess.

One can see that the effective parameters estimated from these simple relations do not deliver good quality solution. It is an expected result since the relations in Fig. 7 were derived

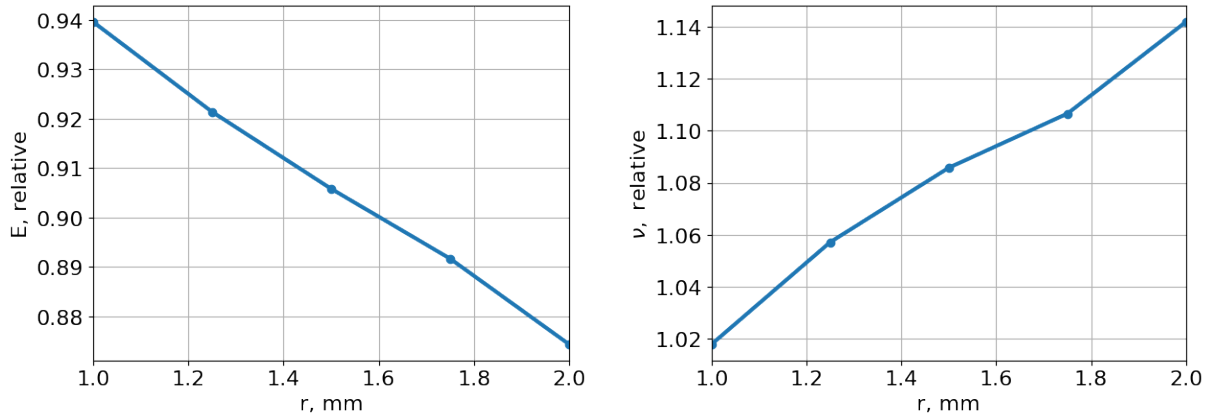


Figure 7. Effective elastic moduli of perforated plate with respect to holes radius: Young's module (left) and Poisson coefficient (right)

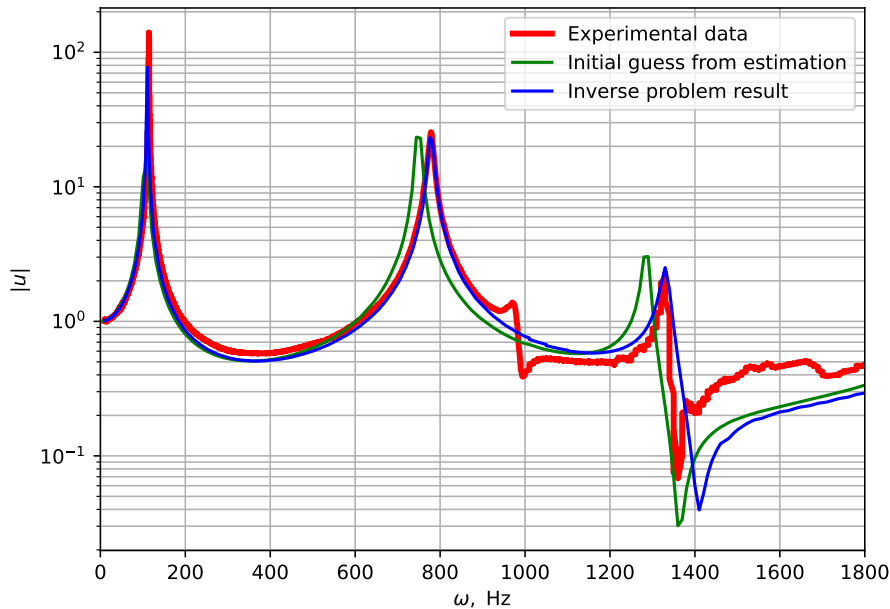


Figure 8. Using perforated plate effective parameters for inverse problem solution

from a sample of certain geometry and rheology, one can not expect that all the specimens from other materials will behave exactly the same. However, these effective parameters can be used as a good initial approximation that reduces the time to final solution.

Conclusion

The present work considers the inverse problem of material elastic properties identification from vibrational testing data. The major focus of the paper is to describe the approach that uses different kinds of optimizations to allow fast inverse problem solution. The methods presented allow to achieve forward problem computation time less than 0.5 seconds using single modern multicore CPU or GPU. This fact makes it possible to solve the inverse problem on a single machine as well. The numerical experiments presented in the paper demonstrate the applicability of the approach for complex rheologies and geometries: multilayered laminated composite plates, isotropic materials with frequency dependent elastic properties, perforated samples.

Several directions, outlined in the present paper, require further research. The inverse problem for thick laminates was solved, but the quality of the solution may be improved. The concept of frequency dependency of elastic moduli should be studied further to become applicable for a larger scope of materials. The approach for perforated specimens effective properties should be refined in future work using the experimental data for different materials.

Acknowledgements

The study was supported by the Russian Science Foundation project № 22-11-00142.

This paper is distributed under the terms of the Creative Commons Attribution-Non Commercial 3.0 License which permits non-commercial use, reproduction and distribution of the work without further permission provided the original work is properly cited.

References

1. Aksenov, V., Vasyukov, A., Beklemysheva, K.: Acquiring elastic properties of thin composite structure from vibrational testing data. *Journal of Inverse and Ill-posed Problems* 32(3), 467–484 (2024). <https://doi.org/10.1515/jiip-2022-0081>
2. Ayyagari, S., Al-Haik, M.: Enhancing the viscoelastic performance of carbon fiber composites by incorporating CNTs and ZnO nanofillers. *Applied Sciences* 9(11), 2281 (2019). <https://doi.org/10.3390/app9112281>
3. Bradbury, J., Frostig, R., Hawkins, P., *et al.*: JAX: composable transformations of Python+NumPy programs. <http://github.com/google/jax> (2018), accessed: 2024-05-30
4. Chaigne, A., Lambourg, C.: Time-domain simulation of damped impacted plates. I. Theory and experiments. *The Journal of the Acoustical Society of America* 109(4), 1422–1432 (2001). <https://doi.org/10.1121/1.1354200>
5. Dagum, L., Menon, R.: OpenMP: an industry standard API for shared-memory programming. *IEEE Computational Science and Engineering* 5(1), 46–55 (1998). <https://doi.org/10.1109/99.660313>
6. Davis, T.A.: Algorithm 832: UMFPACK V4.3 – an unsymmetric-pattern multifrontal method. *ACM Trans. Math. Softw.* 30(2), 196–199 (2004). <https://doi.org/10.1145/992200.992206>
7. Hecht, F.: New development in FreeFem++. *J. Numer. Math.* 20(3-4), 251–266 (2012). <https://doi.org/10.1515/jnum-2012-0013>
8. Jones, R.M.: *Mechanics of composite materials*. Taylor & Francis, Philadelphia, PA (1999). <https://doi.org/10.1201/9781498711067>
9. Kim, S.Y., Lee, D.H.: Identification of fractional-derivative-model parameters of viscoelastic materials from measured FRFs. *Journal of sound and vibration* 324(3-5), 570–586 (2009). <https://doi.org/10.1016/j.jsv.2009.02.040>

10. Koblar, D., Boltežar, M.: Evaluation of the frequency-dependent Youngs modulus and damping factor of rubber from experiment and their implementation in a finite-element analysis. *Experimental Techniques* 40, 235–244 (2016). <https://doi.org/10.1007/s40799-016-0027-7>
11. Lavrenkov, S., Vasyukov, A.: Experimental data compression for GPU-based solution of inverse coefficient problem for vibrational testing data. In: Balandin, D., Barkalov, K., Meyerov, I. (eds.) *Mathematical Modeling and Supercomputer Technologies, MMST 2023*, Nizhny Novgorod, Russia, November 13-14, 2023. Proceedings. Communications in Computer and Information Science, vol. 1914, pp. 302–309. Springer Nature Switzerland (2024). https://doi.org/10.1007/978-3-031-52470-7_24
12. Menard, K.P., Menard, N.: *Dynamic Mechanical Analysis*. CRC Press, Boca Raton, FL (2020). <https://doi.org/10.1201/9780429190308>
13. Morley, L.S.D.: The triangular equilibrium element in the solution of plate bending problems. *Aeronautical Quarterly* 19(2), 149–169 (1968). <https://doi.org/10.1017/S0001925900004546>
14. Nocedal, J., Wright, S.J.: *Numerical Optimization*. Springer New York, New York, NY (2006). <https://doi.org/10.1007/978-0-387-40065-5>
15. Paimushin, V.N., Firsov, V.A., Gazizullin, R.K., Shishkin, V.M.: Theoretical and experimental method for determining the frequency-dependent dynamic modulus of elasticity and damping characteristics of a titanium alloy OT-4. *Journal of Physics: Conference Series* 1158(3), 032044 (2019). <https://doi.org/10.1088/1742-6596/1158/3/032044>
16. Paimushin, V.N., Firsov, V.A., Gyunal, I., Shishkin, V.M.: Accounting for the frequency-dependent dynamic elastic modulus of duralumin in deformation problems. *Journal of Applied Mechanics and Technical Physics* 58, 517–528 (2017). <https://doi.org/10.1134/S0021894417030178>
17. Pritz, T.: Frequency dependences of complex moduli and complex Poisson's ratio of real solid materials. *Journal of Sound and Vibration* 214(1), 83–104 (1998). <https://doi.org/10.1006/jsvi.1998.1534>
18. Rahmani, H., Najaf, S.H.M., Ashori, A., Golriz, M.: Elastic properties of carbon fibre-reinforced epoxy composites. *Polymers and Polymer Composites* 23(7), 475–482 (2015). <https://doi.org/10.1177/096739111502300706>
19. Reddy, J.N.: *Mechanics of Laminated Composite Plates and Shells*. CRC Press, Boca Raton, FL (2003). <https://doi.org/10.1201/b12409>
20. Reddy, J.N.: *Theory and Analysis of Elastic Plates and Shells*. CRC Press, Boca Raton, FL (2006). <https://doi.org/10.1201/9780849384165>
21. Ruzek, M., Guyader, J.L., Pezerat, C.: Experimental identification of the bending equation of beams from the vibration shape measurements. *Journal of Sound and Vibration* 332(16), 3623–3635 (2013). <https://doi.org/10.1016/j.jsv.2013.02.017>

22. Storn, R., Prince, K.: Differential evolution a simple and efficient heuristic for global optimization over continuous spaces. *Journal of Global Optimization* 11(4), 341–359 (1997). <https://doi.org/10.1023/A:1008202821328>
23. Treviso, A., Van Genechten, B., Mundo, D., Tournour, M.: Damping in composite materials: Properties and models. *Composites Part B: Engineering* 78, 144–152 (2015). <https://doi.org/10.1016/j.compositesb.2015.03.081>
24. Tuan, P.H., Wen, C.P., Chiang, P.Y., *et al.*: Exploring the resonant vibration of thin plates: reconstruction of Chladni patterns and determination of resonant wave numbers. *The Journal of the Acoustical Society of America* 137(4), 2113–2123 (2015). <https://doi.org/10.1121/1.4916704>